Supporting Information for

Elucidation of Slow Magnetic Relaxation in a Ferromagnetic 1D Dysprosium Chain through Magnetic Dilution

LiJia[a,b], Qi Chen[a], Yin-Shan Meng[b], Hao-Ling Sun[a]*, and Song Gao[b]*

[a]*Department of Chemistry and Beijing Key Laboratory of Energy Conversion and Storage Materials, Beijing Normal University, Beijing 100875, P. R. China E-mail:* *haolingsun@bnu.edu.cn;*

[b] *Beijing National Laboratory for Molecular Sciences, State Key Laboratory of Rare Earth Materials Chemistry and Applications, College of Chemistry and Molecular Engineering, Peking University, Beijing 100871, China E-mail: gaosong@pku.edu.cn;*

Experimental Section

All the starting materials were commercially available reagents for analytical grade and used without further purification.

[Dy(ppmc)$_2$·4H$_2$O]·ppmc·H$_2$O (1): An aqueous solution (2ml) of Hppmc (0.3mmol) was adjusted to pH=7 with 0.1mol·L^{-1}NaOH solution, then solid Dy(NO$_3$)$_3$·6H$_2$O (0.1mmol) was added and stirred for 10min, producing white precipitate. Then the solvent of water/ethanol (1:1) was added to the mixture and heated until the white precipitate was completely dissolved and filtered. The resultant solution was left unperturbed to allow the slow evaporation of the solvent. Colorless transparent prismatic single crystals, suitable for X-ray diffraction analysis, were formed quickly after 1 day. Yield: 65.0mg (76.4%, based on the metal salt). Elemental analysis (%) calcd for C_{33} H_{31}Dy N_6 O_{11}: C, 46.62, H, 3.68, N, 9.89; found C, 46.90, H, 3.31, N, 10.03. IR (KBr, cm^{-1}):3408(w), 1605(s), 1551(s), 1462(s), 1410(s), 742(s).

[Y(ppmc)$_2$·4H$_2$O]·ppmc·H$_2$O (2): Compound **2** was prepared with the similar method to that of **1**, with only Y(NO$_3$)$_3$·6H$_2$O instead of Dy(NO$_3$)$_3$·6H$_2$O. Yield: 58.0 (74.7%, based on the metal salt).

[Dy$_{0.03}$Y$_{0.97}$(ppmc)$_2$·4H$_2$O]·ppmc·H$_2$O (3): An aqueous solution of Hppmc

(1.5mmol) was adjusted to pH=7 with 0.1mol·L^{-1}NaOH solution. Then 2ml aqueous solution of $Dy(NO_3)_3$/$Y(NO_3)_3$ in 1:50 molar ratio (0.5mmol in total) was added to the solution, and the reaction mixture was stirred for 3h. Three hours later, the solvent of water/ethanol (1:1) 40ml was added to the mixture which was heated until the white precipitate was completely dissolved and filtered. Colorless transparent prismatic single crystals, suitable for X-ray diffraction analysis, were formed quickly after 1 day. Yield: 190.2mg (49.8%, based on $Dy(NO_3)_3 \cdot 6H_2O$).

X-ray crystallography and physical measurement

Intensity data for crystals of **1**, **2** and **3** were collected on a Bruker Smart Apex Ⅱ CCD diffractometer with graphite-monochromated Mo Kα radiation(0.71073 Å) at 296K. The structures were solved by direct methods and refined with the full-matrix least-squares technique based on F^2 usingthe SHELXL program. All non-hydrogen atoms were refined anisotropically. Hydrogen atoms of the water molecules were located from the difference Fourier maps and refined with restraint of the O-H and H···H distances (0.96 and 1.52 Å, respectively). Other hydrogen atoms were placed at the calculation positions. The details of crystallographic data and selected bond parameters for compounds **1**, **2** and **3** are listed in Table S1 and Table S2, respectively.

Elemental analyses of carbon, hydrogen, and nitrogen were carried out with an ElementarVario EL analyzer. FTIR spectra were recorded in the range of 4000 to 400cm^{-1} on an AVATAR 360 Nicolet 380 FT/IR spectrometer using KBr pellets. Powder X-ray diffraction (XRD) analyses were performed on a Rigaku Dmax-2000 X-ray diffractometer with Cu Kα(1.54059 Å) radiation. Variable-temperature magnetic susceptibility measurements of **1** and **3** were performed on an MPMS-7 SQUID and PPMS magnetometer. The experimental susceptibilities were corrected for the diamagnetism of the constituent atoms (Pascal's tables) and background of the sample holder.

Table S1 Crystallographic Data and Structure Refinement for complex **1**, **2** and **3**.

	1	**2**	**3**
Formula	$C_{33}H_{31}DyN_6O_{11}$	$C_{33}H_{31}YN_6O_{11}$	$C_{33}H_{31}Dy_{0.03}Y_{0.97}N_6O_{11}$
Mr	850.14	776．55	778.76
Crystal system	Monoclinic	Monoclinic	Monoclinic
Space group	$P2_1/c$	$P2_1/c$	$P2_1/c$
a(Å)	10.103(1)	10.089(1)	10.082(1)
b(Å)	23.756(2)	23.756(1)	23.728(3)
c(Å)	14.738(2)	14.715(1)	14.719(1)
β (°)	108.424(1)	108.419(1)	108.449(2)
V (Å^3)	3356.0(5)	3346.3(3)	3340.3(6)
Z	4	4	4
μ (mm^{-1})	2.297	1.814	1.832
F(000)	1700	1592	1595
GOF	1.275	1.100	1.020
Data collected	20234	40784	20142
Unique	7700	7671	7696
R_{int}	0.0350	0.0635	0.0431
$R1,wR2[I>2\sigma(I)]$	0.0492,0.1164	0.0600,0.1025	0.0446,0.1037
R1, wR2 [all data]	0.0747,0.1322	0.1043,0.1208	0.0769,0.1149

TableS2. Selected Bond Distances (Å) in Complex **1**.

Ln(1)-O(1)	2.291(4)	Ln(1)-O(2)	2.393(4)	Ln(1)-O(3)	2.292(4)
Ln(1)-O(4)	2.383(4)	Ln(1)-O(7)	2.398(4)	Ln(1)-O(8)	2.364(4)
Ln(1)-O(9)	2.512(4)	Ln(1)-O(10)	2.458(4)		

Table S3. Hydrogen Bonds in **1**.

D-H	d(H···A) (Å)	<DHA(°)	d(D···A) (Å)	A
O7-H7C	1.678	178.81	2.635	O5 [x,y+1,z]
O7-H7D	2.199	139.80	2.994	O10 [-x+1,-y+2,-z+1]
O8-H8C	1.651	169.42	2.589	O6 [x,y+1,z]
O8-H8D	2.052	173.43	2.999	O9 [-x+2,-y+2,-z+1]
O9-H9C	1.922	173.44	2.878	N1
O9-H9D	1.951	147.15	2.809	O11
O10-H10C	1.984	171.59	2.925	N3
O10-H10D	1.824	166.91	2.757	O11
O11-H11C	1.961	139.33	2.764	O5 [-x+1,-y+1,-z+1]
O11-H11D	2.086	143.36	2.909	N6 [-x+1,y+1/2,-z+1/2]

Table S4 Relaxation fitting parameters from Least-Squares Fitting of $\chi(f)$ data under zero dc field.

T (K)	χ_T	χ_S	α	τ (s)
		1		
2.0	8.22	1.51	0.18	6.65E-5
2.5	6.01	1.26	0.17	5.67E-5
3.0	4.47	1.08	0.16	5.12E-5
3.5	3.90	0.95	0.15	4.77E-5
4.0	3.32	0.87	0.14	4.50E-5
4.5	2.88	0.80	0.12	4.20E-5
5.0	2.54	0.70	0.079	3.76E-5
5.5	2.28	0.70	0.040	2.85E-5
6.0	2.07	0.59	0.024	1.69E-5
6.5	1.89	0.43	0.036	8.05E-6
7.0	1.75	0.19	0.072	3.09E-6
		3		
5.0	0.76	0.12	0.16	1.45E-4
5.5	0.68	0.10	0.12	5.33E-5
6.0	0.61	0.0042	0.17	1.47E-5
6.5	0.55	0.020	0.14	5.72E-6

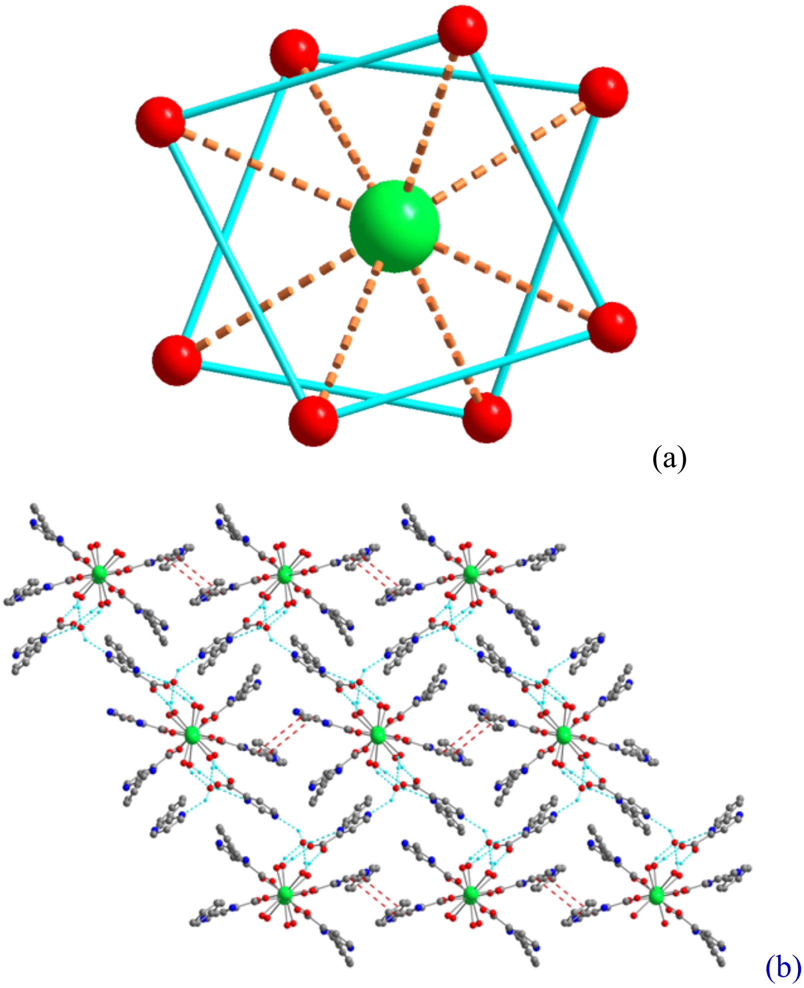

Fig. S1 (a) coordination environment of Dy^{3+} and (b) the 3D supramolecular framework of **1** connected both hydrogen bonds and π-π stacking.

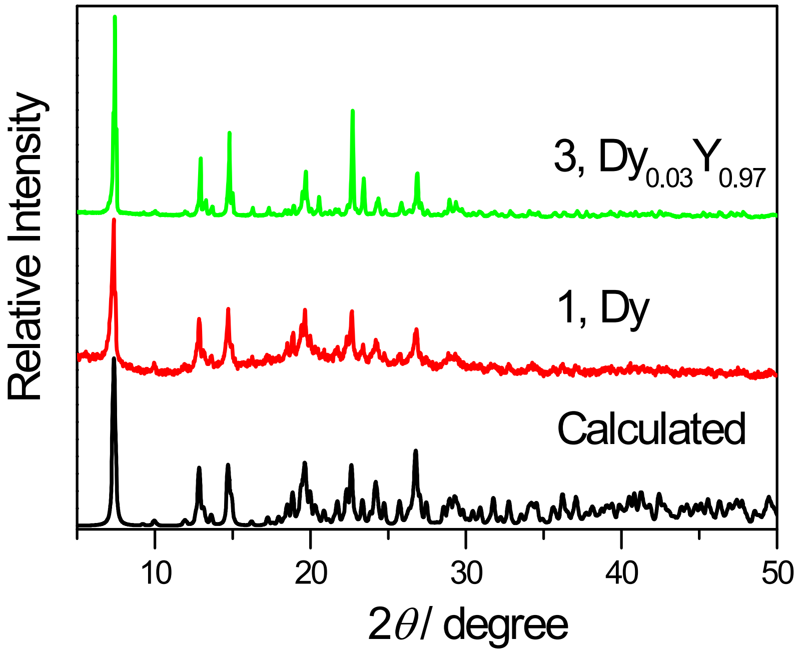

Fig. S2 Powder X-ray diffraction profiles of **1** and **3** together with a simulation from the single crystal data.

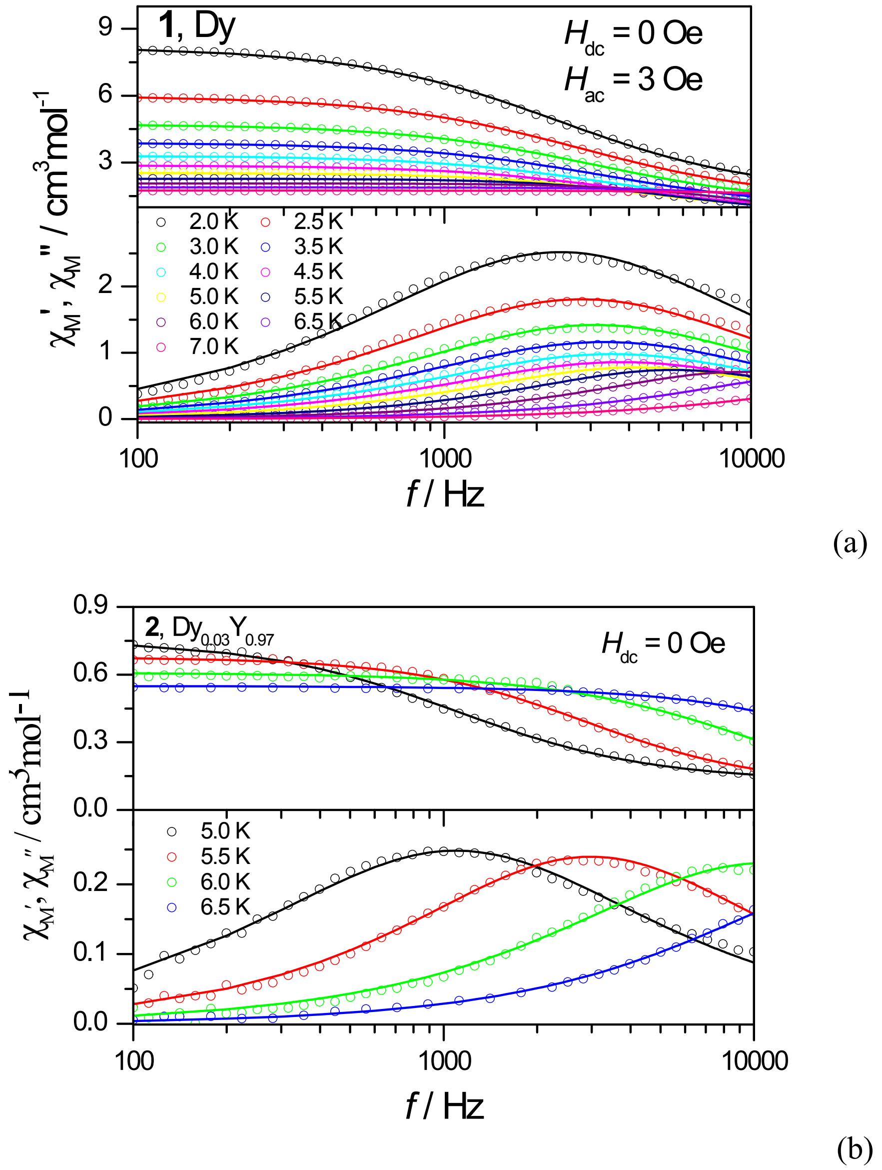

Fig. S3 *Ac-f* curves measured under zero *dc* field for **1** (a) and **3** (b) at selected temperatures. Solid lines were fitted using a generalized Debye relaxation model, simultaneously to χ'(*f*) and χ''(*f*) curves.

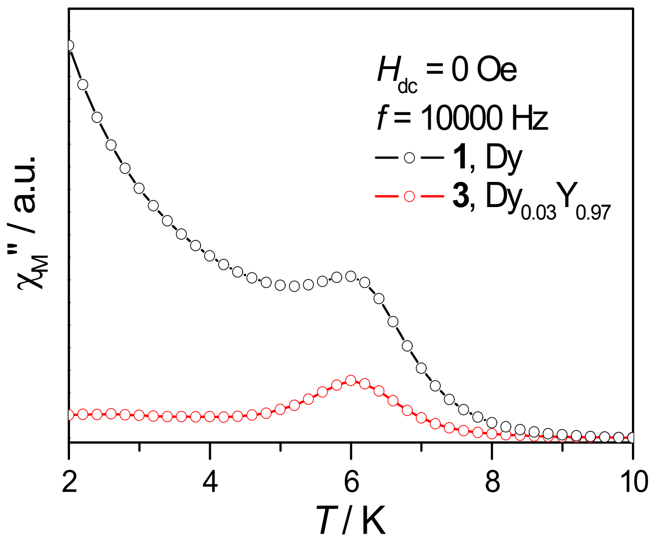

Fig. S4 Temperature dependence of the out-of-phase susceptibility (χ_M'') under zero dc field at 10000 Hz for **1** and **3**.

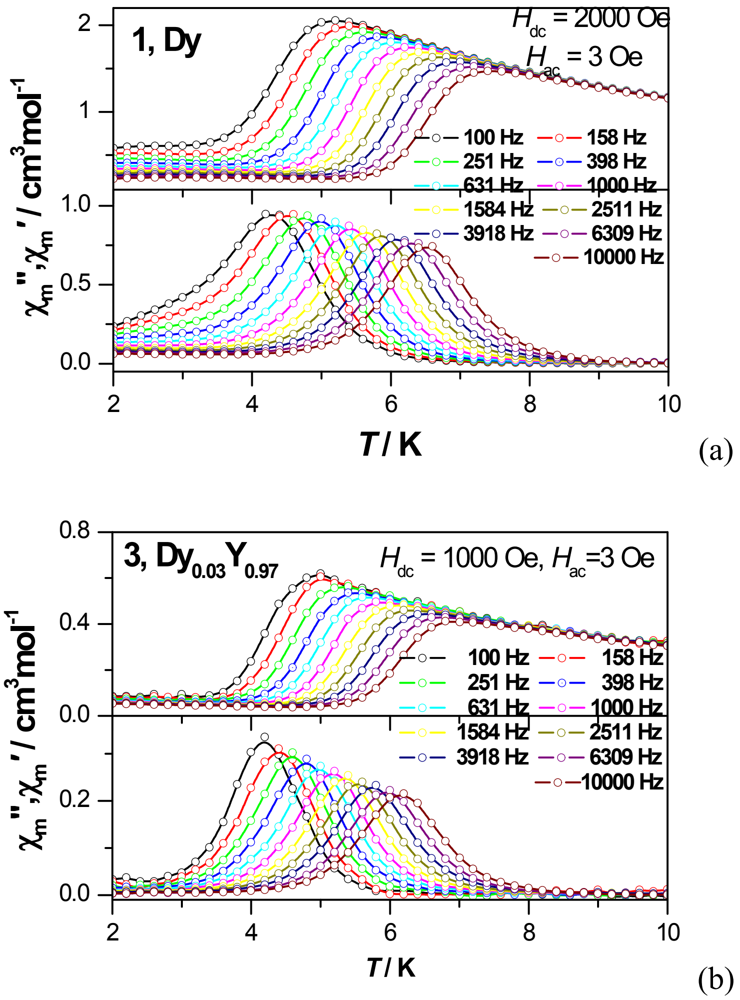

Fig. S5 The temperature dependence of *ac* susceptibility under 2000 Oe field for **1** (a) and 1000 Oe for **3** (b).

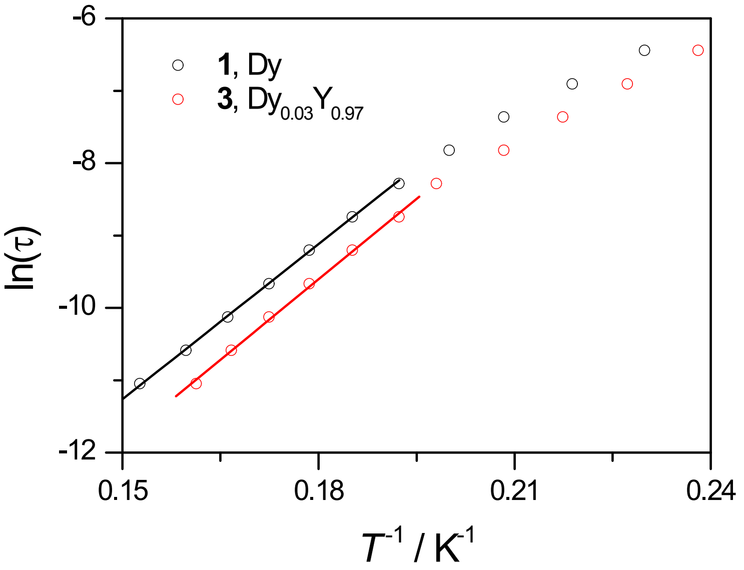

Fig. S6 Plot of ln(τ) versus T^{-1} under 2000 Oe *dc* field for **1** and 1000 Oe *dc* field for **3**. The solid line shows the fitting result by the Arrhenius law.